The membrane-associated form of methane mono-oxygenase from *Methylococcus capsulatus* (Bath) is a copper/iron protein

Piku BASU*[1], Bettina KATTERLE†[1,2], K. Kristoffer ANDERSSON† and Howard DALTON*[3]

*Department of Biological Sciences, University of Warwick, Coventry CV4 7AL, U.K., and †Department of Biochemistry, University of Oslo, P.O. Box 1041, Blindern N-0316 Oslo, Norway

A protocol has been developed which permits the purification of a membrane-associated methane-oxidizing complex from *Methylococcus capsulatus* (Bath). This complex has ≈ 5 fold higher specific activity than any purified particulate methane mono-oxygenase (pMMO) previously reported from *M. capsulatus* (Bath). This efficiently functioning methane-oxidizing complex consists of the pMMO hydroxylase (pMMOH) and an unidentified component we have assigned as a potential pMMO reductase (pMMOR). The complex was isolated by solubilizing intracytoplasmic membrane preparations containing the high yields of active membrane-bound pMMO ($pMMO^m$), using the non-ionic detergent dodecyl-β-D-maltoside, to yield solubilized enzyme ($pMMO^s$). Further purification gave rise to an active complex ($pMMO^c$) that could be resolved (at low levels) by ion-exchange chromatography into two components, the pMMOH (47, 27 and 24 kDa subunits) and the pMMOR (63 and 8 kDa subunits). The purified complex contains two copper atoms and one non-haem iron atom/mol of enzyme. EPR spectra of preparations grown with ^{63}Cu indicated that the copper ion interacted with three or four nitrogenic ligands. These EPR data, in conjunction with other experimental results, including the oxidation by ferricyanide, EDTA treatment to remove copper and re-addition of copper to the depleted protein, verified the essential role of copper in enzyme catalysis and indicated the implausibility of copper existing as a trinuclear cluster. The EPR measurements also demonstrated the presence of a tightly bound mononuclear Fe^{3+} ion in an octahedral environment that may well be exchange-coupled to another paramagnetic species.

Key words: EPR, oxygen activation, particulate methane mono-oxygenase, type 2 copper site.

INTRODUCTION

Methane mono-oxygenase (MMO) is the enzyme responsible for the NADH- and O_2-dependent oxidation of methane to methanol in bacteria. It has been shown to exist in two forms that depend entirely on the level of copper ions in the growth medium [1]. Whereas the copper-independent soluble form of MMO (sMMO) has been well characterized [2–9] the copper-containing membrane-associated particulate form of MMO (pMMO) has proved less tractable and has given rise to a number of conflicting reports over the last 25 years concerning its structural and mechanistic characteristics [10–30].

Smith and Dalton [31] were the first to partially purify pMMO from *Methylococcus capsulatus* (Bath), using the non-ionic detergent dodecyl-β-D-maltoside to solubilize the enzyme. The enzyme was found to consist of polypeptides of masses 49, 23 and 22 kDa [31]. The 23 kDa subunit was shown to bind acetylene [32], a powerful inhibitor of MMO activity [33], and was presumed to be the site of methane activation. Using duroquinol [34] as the reductant, Zahn and DiSpirito [30] purified the complex from *M. capsulatus* (Bath) under anaerobic conditions. They found that the enzyme consisted of three polypeptides of molecular masses 46, 27 and 25 kDa, which contained 14.5 copper and 2.5 iron atoms/99 kDa of enzyme, and had a specific activity of ≈ 11 nmol/min per mg. Two other polypeptides (37 and 20 kDa) that co-purified with the pMMO were identified as cytochrome *b*-559/569. Efforts to remove these polypeptides resulted in a total loss of activity. They also observed copper-binding cofactors of molecular mass 618 Da, associated with the pMMO, which were believed to have a role in sequestering copper [30].

The enzyme purified by Nguyen et al. [16] had low specific activities of 2–5 nmol of propylene oxide produced/min per mg with ≈ 12–15 Cu atoms/94 kDa monomeric unit but no iron was detected in these preparations. Preparations of pMMO from another methanotroph, *Methylosinus trichosporium* OB3b [20,22], have also been reported. The molecular mass of the OB3b enzyme was estimated to be 326 kDa by gel filtration and was comprised of two subunits with molecular masses of 25 and 41 kDa, with a trace of a contaminating polypeptide (26 kDa). The enzyme was found to contain 0.9 iron atoms and 12.8 copper atoms/molecule.

Since copper was shown to be an important constituent of the preparations and indeed acts as a stimulant of pMMO activity [35], EPR measurements have been used to determine the role of metals in the hydroxylase component. Chan and co-workers [11,16–19] observed a type 2 copper EPR signal in their pMMO samples. When pMMO was oxidized with ferricyanide the sample gave rise to a broad isotropic signal which was proposed to be due to a trinuclear copper cluster presumably arranged in between five and seven mixed-valence clusters. They postulated that these trinuclear copper clusters could be classified into two groups according to their role in catalysis (C-clusters) and electron

Abbreviations used: ICM, intracytoplasmic membrane; ICP-ES, inductively coupled plasma-emission spectroscopy; MMO, methane mono-oxygenase; pMMO, particulate MMO; sMMO, soluble form of MMO; pMMOH, hydroxylase component of pMMO; pMMOR, reductase component of pMMO; $pMMO^c$, pMMOH–pMMOR complex; $pMMO^m$, membrane-bound pMMO; $pMMO^s$, solubilized pMMO; PMS, phenazine methosulphate.

[1] These authors contributed equally to this work.

[2] Present address: Max Planck Institute of Radiation Chemistry, Stiftstr. 34-36, D45470 Mülheim/Ruhr, Germany.

[3] To whom correspondence should be addressed (e-mail HDalton@bio.warwick.ac.uk).

transfer (E-clusters). The two or three C-clusters were proposed to function as the catalytic core of the enzyme and the three or four E-clusters were presumed to be the source of endogenous reducing equivalents [17]. Similar findings were also reported by Takeguchi and co-workers [20,36], who also concluded that a trinuclear copper cluster model fitted with their data for pMMO from *Me. trichosporium* OB3b.

Zahn and DiSpirito [30] presented an alternative model in which enzyme catalysis involved both a copper and an iron species. Their EPR parameters were consistent with a type 2 copper centre ($g_{\parallel} = 2.26$ and $g_{\perp} = 2.06$, $A_{\parallel}^{Cu} = 18.0$ mT, $A^{N} = 1.5$ mT), but also gave a weak high-spin iron signal ($g = 6.0$) and a broad low field signal at $g = 12.5$ which was lost when the sample was reduced by dithionite or ascorbate. They also suggested that the loosely bound copper ions associated with copper-binding cofactors may be responsible for the broad isotropic signal observed by Chan and co-workers [11,16–19]. The presence of iron in the enzyme was also supported by the observation of copper-induced iron uptake into the membranes, activation of pMMO by ferric ions in purified preparations of *M. capsulatus* (Bath) and the formation of the NO–ferrous iron complex. X-band and S-band EPR studies on whole cells and membranes from *M. capsulatus* (Bath) and *Methylomicrobium album* BG8 [15,26–29] suggested the presence of two nearly identical type 2 copper signals in whole cells of both organisms. The second signal found in membrane fractions was attributed to the oxidation of cupric sites. The S-band EPR spectra gave resolved N hyperfines in the $g_{\perp}$ region and established unambiguously that one cupric ion was ligated to four nitrogen donor atoms. Furthermore there was no evidence for iron in pMMO from *Meth. album* BG8 cells.

There is clearly some debate over the exact nature of the copper ions and indeed whether iron plays any role in the active site of pMMO, since Chan and co-workers believe that its presence is due to contamination [16]. One possible cause of this variation in the presence and structure of the metals at the active site of the enzyme may well stem from the low-activity forms, purity and the variation in specific activity reported for the different preparations. Here we report a method of purification that has given rise to material of high specific activity, and we have investigated the nature of the active site using EPR methods. The purification protocol developed here has also led to the possible identification of an enigmatic component of the methane-oxidizing complex that may link NADH oxidation to the hydroxylase.

MATERIALS AND METHODS

Growth and maintenance of micro-organisms

Methanotrophs were grown in nitrate minimal salts medium [37]. A final $CuSO_4$ concentration of 1.5 mg/l was used in the trace elements solution when pMMO-expressing cells were grown.

Batch fermentation of *M. capsulatus* (Bath)

Large-scale batch fermentation of *M. capsulatus* (Bath) was performed in a 100 l fermenter (LH Engineering, Stoke Poges, Bucks., U.K.). Nitrate minimal salts medium was supplemented with an additional 1.0 g/l KNO_3 to prevent cells from becoming nitrate-limited during the later stages of growth. The fermenter was inoculated with 10 l of cells from a continuous culture overflow. Methane was provided as a methane/air mixture (20 %, v/v, in air). Cells were harvested after a D_{550} value of 7 was obtained (for pMMO-expressing cells) by centrifugation at 3000 ***g*** in a Westfalia continuous centrifuge (Westfalia Separator, Milton Keynes, U.K.).

Table 1 Specific activities of pMMO from *M. capsulatus* (Bath) at different stages of a typical purification run

Activity measurements were made using the standard propylene to propylene oxide detection. Measurement of the activity of pMMO[c] was assayed using the optimized conditions. Specific activity was measured using duroquinol as the electron donor.

Stage of pMMO purification	Total protein (mg)	Activity (nmol of propylene oxide produced/min)	Specific activity (nmol of propylene oxide produced/min per mg)	Yield (%)
ICMs	300	5700	19	100
After solubilization	150	4550	30	79
After Superdex 200	70	3150	53	55

Preparation of pMMO-containing extracts

Cell paste from the 100 l fermenter expressing pMMO was resuspended in 25 mM Pipes buffer, pH 7.25, centrifuged at 10000 ***g*** for 15 min at 4 °C and resuspended in the same buffer. DNase I (1 mM) and benzamidine (1 mM) were added to the cell suspension and the cells were then broken by two to three passes through a Constant cell disrupter (Constant Systems, Warwick, U.K.) at 25 kPa until a smooth paste was obtained. Unbroken cells and cell debris were removed by centrifugation at 10000 ***g*** for 30 min at 4 °C.

Isolation of intracytoplasmic membrane (ICM)

ICMs were collected by centrifugation at 150000 ***g*** for 60–90 min (depending on volume) at 4 °C and the pellet containing the ICMs was resuspended in 25 mM Pipes, pH 7.25, containing 0.5 M NaCl and 1 mM benzamidine. This process was repeated at least twice to remove soluble proteins until the supernatant was clear, before finally resuspending the pellet in 25 mM Pipes, pH 7.25, 0.5 M NaCl and 1 mM benzamidine. The membrane-bound pMMO extract (pMMO[m]) was then drop-frozen in liquid nitrogen and stored at −80 °C.

Solubilization of ICMs

The particulate extract was thawed and extracts with high specific activities (> 75 nmol of propylene oxide produced/min per mg of protein; see Table 1) and consisting of at least 60 % of the polypeptides associated with pMMO (as analysed by SDS/PAGE) were used for the solubilization stage. The extract was centrifuged at 150000 ***g*** for 30 min at 4 °C. The pellet was resuspended in a freshly made up buffer of 25 mM Pipes, pH 7.25, 0.5 M NaCl and 1 mM benzamidine. $CuSO_4$ was added to give a final concentration of 40 μM.

Solubilization was performed by adding the dissolved anionic detergent dodecyl-β-D-maltoside (Ultrol grade; Calbiochem, CA, U.S.A.) to give a detergent/protein (w/w) ratio of 1.5 to the particulate extract. The detergent was added drop-wise while stirring constantly on ice. The particulate extract was then left for 1 h on ice with continuous but gentle stirring. After this time

the extract was centrifuged at 150000 ***g*** for 90 min. The solubilized extract was assayed for propylene-oxidizing activity using duroquinol as the reductant. Solubilized pMMO (pMMO^s) extracts were drop-frozen in liquid nitrogen and stored at −80 °C.

Purification methods

Chromatographic procedures for protein purification were performed on a Pharmacia FPLC Basic system, complete with two P-500 pumps, an LCC 500 programmable pump controller, a monitor UV-M detector system and a FRAC-100 fraction collector. The chromatographic media were packed into Pharmacia XK columns. All FPLC columns were washed with two column volumes of degassed distilled water before equilibrating with the appropriate buffer before each purification run. Superdex 200 preparative-grade columns (Amersham Biosciences), either XK 26/600 (2.6 cm × 68 cm) or XK 16/200 (1.5 cm × 68 cm), were used.

Isolation of pMMO^c, the complex of the hydroxylase (pMMOH) and reductase (pMMOR) components of pMMO

pMMO^s was concentrated using an Amicon stirred cell with an XM50 filter (Amicon Corporation, Danvers, MA, U.S.A.) to 20 mg/ml (further concentration at this stage can lead to precipitation). The concentrated extract was then filtered through a 0.2 μM Whatman syringe filter and applied to a pre-cooled (4 °C) Superdex 200 column (1.5 cm × 68 cm) equilibrated with 25 mM Pipes buffer, pH 7.25, supplemented with 0.03 % dodecyl-β-D-maltoside and 1 mM benzamidine. The column was run at a flow rate of 1.5 ml/min.

Fractions containing pMMOH were pooled from the gel-filtration column (Superdex 200) and concentrated using an Amicon stirred cell concentrator with an XM50 filter membrane to give > 50 mg of protein/ml. The sample was then drop-frozen in liquid nitrogen and stored at −80 °C until further use. The sample could then be analysed by electron microscopy to ensure complex homogeneity.

Separation of components of pMMO^c

A DEAE-cellulose DE52 ion-exchange column (Whatman; 1.5 cm × 15 cm) was used to separate pMMO^c into its constituents. Concentrated pMMO^c obtained from the Superdex 200 column (> 15 mg/ml) was filtered through a 0.2 μM syringe filter and applied to a cooled (4 °C) DE52 column which was equilibrated in 10 mM Pipes buffer, pH 7.25, supplemented with 0.01 % dodecyl-β-D-maltoside and 1 mM benzamidine. The flow rate of the column was 2 ml/min. Fractions corresponding to the hydroxylase and the reductase were collected during the washing step and concentrated using an Amicon stirred cell with a PM10 ultrafiltration membrane. An increasing salt gradient was applied to elute undissociated complex.

Cell extract MMO assays

MMO activity in cell extracts was determined following the oxidation of propylene to propylene oxide using NADH or duroquinol as the electron donor. Samples (10 mg/ml) were placed in a 2 ml vial containing the appropriate buffer (25 mM Mops buffer, pH 7, for sMMO extracts and 10 mM Pipes buffer, pH 7.25, for the pMMO) in a final volume of 100 μl. The flask was sealed and 0.5 ml of air was replaced with 0.6 ml of propylene. The flask was then incubated in a 45 °C water bath for 1 min before NADH or duroquinol was added to give a final concentration of 5 M. The gas-phase sample (0.5 ml) was injected on to the GC column to assay for propylene oxide formation using a Pye Unicam Series 104 gas chromatograph (Pye Unicam, Cambridge, U.K.) fitted with a Porapak Q column (4 mm × 1 m; Waters Associates, Milford, MA, U.S.A.). Nitrogen was used as the carrier gas at a flow rate of 30 ml/min and oven temperatures of 150–200 °C. A 2 mM standard of propylene oxide under identical conditions to the assay system was used to calibrate the column.

Activity assays for pMMO^s and pMMO^c

The electron donor used in these assays was 5–25 mM duroquinol. Duroquinol was dried on to the base of a 2 ml vial. The protein sample and 10 mM Pipes buffer, pH 7.25, was added to give a final volume in the vial of 100 μl. Then 0.6 ml of air was extracted from the vial and 1 ml of propylene was injected into it. The reactions were supplemented with 50 μM $CuSO_4$ to give optimal activity.

Quinol preparation

Duroquinone (tetramethyl-*p*-benzoquinone) was obtained from Sigma and was reduced to the corresponding quinol using a 1.5-fold molar excess of solid $NaBH_4$ [34].

Analytical determinations

Protein concentration

Protein concentrations were estimated using a modified dye-binding method of Bradford [38] with BSA as a standard. An alternative assay modified from that described by Lowry et al. [39] was used, which was more suitable for detergent-containing samples. Both procedures were carried out using the Bio-Rad reagent and the detergent-compatible reagent (Bio-Rad, Watford, Herts., U.K.).

Quantification of metal content

Quantification of the copper and iron contents of samples was performed by using inductively coupled plasma-emission spectroscopy (ICP-ES) at the Warwick Analytical Centre, University of Warwick, Coventry, U.K. Samples were prepared by acid washing in nitric acid (Primar grade). A control sample of buffer alone was also prepared in the same way and values obtained for this control were subtracted from the experimental protein sample values.

EPR spectroscopy

Low-temperature experiments (4–10 K) were carried out with a Bruker ESP300 spectrometer operating at X-band frequency (9.6 GHz) and equipped with a cryogenic assembly consisting of an ER900 Oxford Instruments liquid helium cryostat. The copper concentration of the pMMO samples was obtained by double integration and comparison with a 1 mM $Cu(ClO_4)_4$ standard. The signal at $g = 4.3$ was compared with a 1 mM transferrin standard. The EPR spectra were simulated with WinSimfonia (Bruker). Evaluation of the power of half saturation, $P_{1/2}$, from microwave power saturation curves was performed as described by Sahlin et al. [40]. The protein concentration of extracts used in EPR experiments varied. Final sample volumes of 200 μl were used and were frozen slowly in EPR tubes at −190 °C.

Reduction experiments

For the reduction experiments 1 mM ascorbate or 1 mM dithionite was used, plus 500 μM phenazine methosulphate (PMS) as the mediator. The experiments were performed in an anaerobic chamber while flushing with argon. The pMMO^{c} concentration was $\approx$ 5 mg/ml. The samples were incubated 10 min before freezing. To detect any mixed-valency di-iron cluster the pMMO^{c} was placed in an EPR tube, which was evacuated and then flushed with argon several times to obtain anaerobic conditions. Ascorbate and PMS were then added as anaerobic solutions and the sample was incubated for 10 min prior to freezing and EPR measurements.

EDTA treatment and copper titration

The pMMO^{c} samples were washed twice with 10 mM EDTA, 10 mM Pipes, pH 7.25, and 0.03 % dodecyl-β-D-maltoside before final washing with 10 mM Pipes, pH 7.25, and 0.03 % dodecyl-β-D-maltoside. Samples were washed by centrifugation in a Centricon 10 centrifuge (Amicon Corporation) at 3000 ***g*** and 4 °C.

The copper titration experiment was performed in an EPR tube with a 160 μl sample containing 5 mg/ml pMMO^{c}. An aliquot of an appropriate $CuCl_2$ stock solution in water was added to the protein sample. The sample was incubated for 5 min, frozen in liquid nitrogen and then an EPR spectrum under non-saturating conditions was recorded. At the end of the titration at 157 μM Cu^{2+} the protein sample was loaded on to a Sephadex G-25-packed disposable column (1 ml volume) equilibrated with 10 mM Pipes, pH 7.25, and 0.03 % dodecyl-β-D-maltoside. The column was centrifuged for 3 min at 4500 ***g*** in a bench top microfuge, yielding an undiluted, desalted protein sample. The added copper was removed completely after this desalting step.

RESULTS AND DISCUSSION

Enzyme purification

Despite many attempts using published protocols [16,30], we were unable to obtain preparations with specific activities of pMMO^{s} in excess of 10 nmol of propylene oxidized/min per mg protein. We finally devised a protocol that depended on improvements at all stages of purification, giving rise to a highly efficient duroquinol-driven particulate methane-oxidizing complex.

We found that in 100 l batch cultures it was essential to use only fast-growing cells (doubling time < 5 h), which generally produced high-specific-activity pMMO membrane preparations (75–200 nmol/min per mg when using NADH as the reductant; 19 nmol/min per mg when using duroquinol as the reductant). MMO active cultures were verified to be free of sMMO contamination by Western blot analysis using antibodies raised to the sMMO polypeptides, and by naphthalene assay (a measure of soluble MMO activity [41]).

Membrane isolation

Since the pMMO activity was located on the ICMs of the cell it was essential to remove outer membranes and soluble or periplasmic proteins by the use of several ultracentrifugation steps and ionic washes, as described in Materials and methods section. The procedure yielded pMMO^{m} which were estimated to contain $\approx$ 60 % of the polypeptides associated with the pMMOH, as judged by SDS/PAGE. Furthermore the stringent washing protocol removed high-molecular-mass and soluble proteins as observed by electron microscopy of membranes.

Certainly the 'as isolated' activity of pMMO in the membrane preparations (50–200 nmol/min per mg when using NADH as a reductant) is at least an order of magnitude lower than the whole cell activity (up to 2000 nmol/min per mg). It is also clear that the washed membrane preparations are enriched with pMMO; i.e. $\approx$ 60 % of the total proteins were identified as the polypeptides associated with the pMMOH and gave rise to activities in excess of 75 nmol/min per mg when using NADH as a reductant.

Solubilization of pMMO^{m} to give pMMO^{s}

Previous studies with various detergents [31] concluded that dodecyl-β-D-maltoside was the only detergent to yield an active pMMO enzyme and was the detergent of choice in this study. The active pMMO^{m} was solubilized using 1.5 mg of dodecyl-β-D-maltoside/mg of protein and 40 μM $CuSO_4$. However, this detergent/protein ratio was only effective when the membrane pellet was repeatedly resuspended in buffer containing an optimal NaCl concentration of 0.5 M prior to solubilization. We suggest that a stringent salt (0.5 M) washing procedure may stabilize interactions within the protein complexes, allowing an intact and therefore active methane-oxidizing complex to be solubilized. It may also be essential in removing contaminating proteins that may either serve to deflect reductant away from the hydroxylase or may inhibit activity directly. This process yielded pMMO^{s} with specific activities that were up to 5-fold higher than previously reported [16,30] in the range of 15–30 nmol of propylene oxide produced/min per mg of protein. It is important to note that at this stage the solubilized pMMO^{c} could no longer use NADH as a reductant. Instead the plastoquinol analogue duroquinol was used, as described previously by Shiemke et al. [34]. Any attempts to reproduce the purification under anaerobic conditions were unsuccessful, resulting in low activity (5–10 nmol of propylene oxide produced/min per mg of protein) or inactive samples.

Solubilization of the membranes with dodecyl-β-D-maltoside also served as a highly effective initial purification step, resulting in $\approx$ 75 % of the total proteins being identified as the polypeptides associated with pMMOH.

Isolation of pMMO^{c} and its components, pMMOH and pMMOR

The pMMO^{s} extract was applied to a Superdex 200 gel-filtration column. Activity assays were used to confirm which fractions contained pMMO. The active fractions contained $\approx$ 90 % of the polypeptides associated with the pMMOH and an additional component of approximate molecular mass of 63 kDa, as analysed by SDS PAGE (Figure 1, lane 2). However, electron microscopy analysis indicated that there was complex heterogeneity in the sample. From this it could be inferred that the 63 kDa component was associated with the pMMOH in a complex which we now refer to as pMMO^{c}.

Activities obtained for the pMMO^{c} were found to be $\approx$ 5-fold higher than previously reported values and were in the range of 30–75 nmol/min per mg when using duroquinol as the reductant. Specific activities of pMMO using duroquinol as the reductant during a typical purification run are shown in Table 1.

Since this was the first report of an active duroquinol-driven complex containing the pMMOH and an additional component of $\approx$ 63 kDa, it was necessary to assess whether the latter had any role to play in pMMO activity or was simply a contaminant bound to pMMOH. It was therefore necessary to isolate the

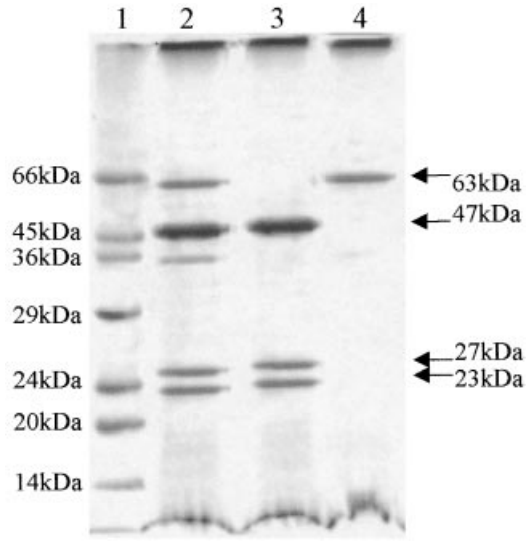

Figure 1 SDS/PAGE (12% gel) showing peaks collected from anion-exchange DEAE-cellulose column

Lane 1, Sigma Dalton-II molecular-mass markers. Lane 2, pMMO^c from a Superdex 200 column (5 μg). Lane 3, pMMOH from DEAE-cellulose column (5 μg). Lane 4, pMMOR from DEAE-cellulose column (5 μg). Proteins were visualized by staining with Coomassie Brilliant Blue R-250.

unknown component from the hydroxylase so that initial characterization could be made.

Limited resolution of pMMO^c into its components was obtained using anion-exchange chromatography (DEAE-cellulose), probably due to the stability of the complex. The resolved components were found to consist of the pMMOH (Figure 1, lane 3) and the 63 kDa component (Figure 1, lane 4). Further analysis of the 63 kDa sample by MS identified the presence of another polypeptide of 8 kDa. The co-purification of these polypeptides indicates that they exist together as a complex.

The existence of the pMMOH has been established previously. It has also been suggested before that there may be extra component(s), e.g. a reductase necessary for the efficient functioning of an active particulate methane-oxidizing complex. This suggestion is upheld by the reports of low specific activities of the purified pMMO of $\approx$ 10 and 2.6–5 nmol/min per mg by other groups [16,30]. Since the component containing the 63 and 8 kDa subunits co-purified with pMMOH, it was nominated as a potential candidate for the reductase pMMO complex and therefore designated pMMOR. Initial characterization of the pMMOR was carried out to assess if this unknown component had any role in supporting pMMO activity.

Reconstitution of the pMMO^c components

The pMMO^c and its individual components were assayed for activity (Table 2) using duroquinol as a reductant. Neither the pMMOH nor the pMMOR could support any MMO activity individually. This would indicate that both are necessary for propylene-oxidizing activity in the complex. When the isolated pMMOH and pMMOR were added back to the purified pMMO^c the activity increased but the specific activity (28 nmol of propylene oxide produced/min per mg) remained approximately the same. However, the reconstitution of the complex by the addition pMMOH and pMMOR in the absence of complex, yielded only 10% of the activity of the as-isolated pMMO^c.

Table 2 Specific activities of reconstituted proteins

pMMO assays were carried out by the detection of propylene oxide production using 10 mM Pipes, pH 7.25, 25 mM duroquinol and 0.05 mM $CuSO_4$. Results are means $\pm$ S.D. from at least two measurements.

Sample	Total protein (mg)	Mean activity (nmol of propylene oxide/min)	Specific activity (nmol of propylene oxide/min per mg)	Activity (%)
pMMO^c	0.5	13.75 $\pm$ 0.25	27.5	100
pMMO^c + pMMOH	0.6	17.15 $\pm$ 0.45	28.6	105
pMMO^c + pMMOR	0.6	16 $\pm$ 5	26.6	100
pMMOH + pMMOR	0.5	1.3 $\pm$ 0.6	2.6	9.5
pMMO^c + pMMOH + pMMOR	0.7	19 $\pm$ 3	27.1	95
pMMOH	0.5	0	0	0
pMMOR	0.5	0	0	0

The fact that the pMMOH cannot support activity without pMMOR indicates that the pMMOR is a necessary constituent for an active duroquinol-driven particulate methane-oxidizing complex. The failure to reassemble an efficiently functioning complex (i.e. activity at only 10% of the original activity) from individual components may indicate that other non-protein components, e.g. haem prosthetic groups or metal cofactors, removed during their purification may also be required to obtain optimal activity. The exact functional impact of the pMMOR on the pMMOH can only be established once an optimized reconstitution protocol has been established. This process was hindered by the restrictively low yields of individual components isolated during the study, due to the complex stability. However, further characterization of the pMMO^c could be carried out to determine the metal centre of this pMMO^c (see below).

The isolation of a component that may be the pMMO reductase is not unprecedented, as it has been suggested that high pMMO activities can be obtained when a purified NADH reductase is added back to the activity assay [16]. As yet there has been no published procedure to confirm the existence and subsequent isolation of an NADH reductase. Shiemke and co-workers [34] also observed that the addition of catalytic amounts of exogenous quinones to solubilized extracts could restore the role of NADH as a reductant of pMMO. This indicated that an NADH:quinone oxidoreductase might be involved in the reduction of pMMO by NADH *in vivo*. They also claimed to have purified small amounts of a NADH:quinone oxidoreductase (36 kDa) which was thought to mediate this reaction, although there have been no subsequent reports on the isolation of this enzyme.

Our attempts to drive the MMO reaction with NADH, pMMOH and pMMOR were unsuccessful. The inability of the complex to use NADH as a reductant suggests the disruption of the electron transport chain from NADH to the pMMO. The similarity in subunit size between our pMMOR component and the NAD-linked formaldehyde dehydrogenase from *M. capsulatus* (Bath) [42] has been noted. In addition to this, the N-terminal sequence of the 63 kDa component (NGELDRNSKG) was found to share high homology with the NAD-linked formaldehyde dehydrogenases and various methanol dehydrogenases. The mechanism by which the component functions in the *in vivo* electron transfer to the pMMO could be based on the same basic principles proposed by Tonge et al. [23]. However, attempts to use methanol or formaldehyde to drive the pMMO reaction were unsuccessful and this may be due to the absence of another component, such as a cytochrome, as suggested originally by Tonge et al. [23]

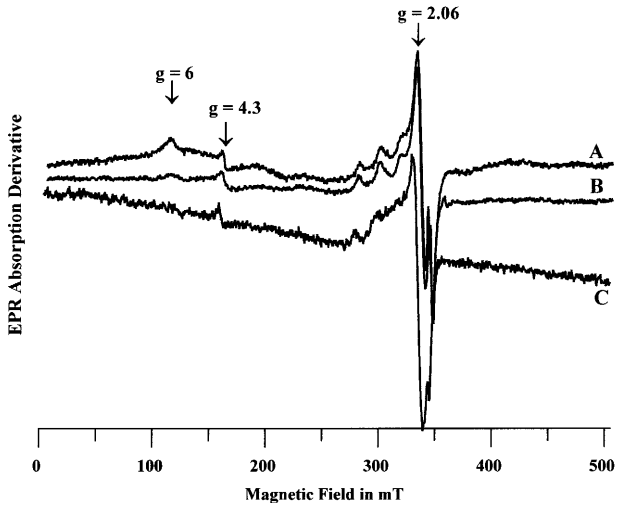

Figure 2 X-band EPR spectra of pMMO^{m}, pMMO^{s} and pMMO^{c} of *M. capsulatus* (Bath)

pMMO^{m} had a concentration of 27 mg/ml (trace A), pMMO^{s} of 15 mg/ml (trace B) and the purified pMMO^{c} of 5 mg/ml (trace C). Spectra were recorded at a microwave power of 10 mW, a modulation frequency of 100 kHz, a temperature of 10 K and a modulation amplitude of 0.5 mT.

(cytochrome *c*) and more recently by Zahn and DiSpirito [30] (cytochrome *b*). The purification of this membrane-associated methane-oxidizing complex may provide us with a better insight into the possible *in vivo* mechanism of electron transfer to pMMO.

The nature of the EPR active copper ions in pMMO

Low-temperature EPR spectroscopy (9.6 GHz) was used to examine different pMMO preparations for possible copper, iron or other EPR active signals (Figure 2). The EPR signals from pMMO^{m} and pMMO^{s} preparations were partially microwave-power-saturated, but still very informative. The type 2 Cu^{2+} EPR

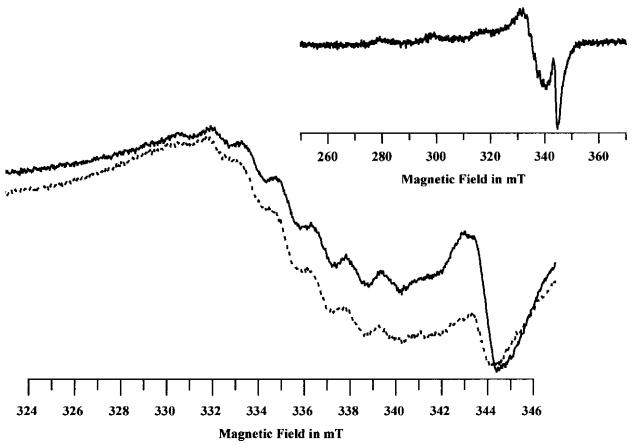

Figure 3 EPR spectra of pMMO^{c} purified from *M. capsulatus* (Bath) cells grown in ^{63}Cu-enriched media

The ^{63}Cu-enriched media (dotted trace) and non-enriched media (solid trace). pMMO^{c} samples had a concentration of 5 mg/ml. The inset shows the whole type 2 copper spectrum of pMMO^{c}. Spectra were recorded as detailed in Figure 1.

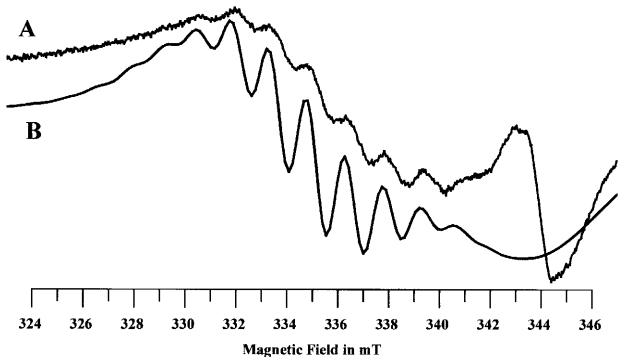

Figure 4 Comparison of the experimental cupric signal at $g_{\perp}$ from pMMO^{c} with a simulation consistent with mononuclear type 2 copper parameters

At $g_{\perp}$ shown here the A^{N}-superhyperfine interactions are well resolved. Trace A, copper EPR signal of pMMO^{c} from *M. capsulatus* (Bath) from this study; trace B, simulation of the EPR spectrum. The simulated EPR parameters of pMMO^{c} are $g_{\parallel} = 2.24$, $g_{\perp} = 2.06$, $A_{\parallel}^{Cu} = 18.5$ mT and four equivalent $A^{N} = 1.5$ mT. Spectra were recorded as detailed in Figure 1.

spectra, observed between 26 and 36 mT, indicated that the solubilization of ICMs did not influence the ligand environment of the EPR-active cupric site(s). Both samples displayed spectra with an axial copper signal, which is indicative of a type 2 Cu^{2+} signal with square planar geometry. The $g_{\perp}$ region at $g = 2.06$ gave resolved hyperfine signals ($A^{N} = 1.5$ mT), which are due to interactions with nitrogenic ligands [$I(^{14}N) = 1$; see below].

Other EPR signals were observed at $g = 6$, which was assigned to a high-spin ferric signal (possibly a cytochrome), and a broad rhombic ferric signal at $g = 4.3$, which is characteristic of non-specifically bound Fe^{3+} ions. The relative concentration of these $g = 4.3$ and $g = 6$ signals were low when compared with the Cu^{2+} signal. A small signal ($< 3\ \mu$M) at $g = 2.0$ (near 33.4 mT in Figures 3 and 4) was also observed which is indicative of an organic radical, probably a semiquinone species. Typically the specific activities of pMMO^{m} and pMMO^{s} were 19 and 30 nmol of propylene oxide produced/min per mg when using duroquinol as a reductant, suggesting that the solubilization of the pMMO did not perturb the metal-ion-dependent centres and that the EPR signals obtained were those associated with the active protein.

EPR spectra of pMMO^{c} isolated from ^{63}Cu-enriched cells

M. capsulatus (Bath) and *Meth. album* BG8 cells, grown on both ^{63}Cu- and ^{15}N-enriched media, were used to unambiguously identify X-band and S-band EPR cupric signals that corresponded to a Cu^{2+} ion ligated to four nitrogens based on analysis of the superhyperfine couplings from nitrogen [15,26,28]. Our *M. capsulatus* (Bath) cells were grown in ^{63}Cu-enriched media to avoid superposition of signals from ^{63}Cu and ^{65}Cu, to try and establish conclusively whether the superhyperfine splittings (A^{N}) observed in the EPR-visible cupric site of pMMO were consistent with the spectrum for one or two mononuclear type 2 copper(s) and to identify the ligand environment.

In pMMO^{c} the signals at $g = 6$ and $g = 2.0$ were not usually observed (Figure 2, trace C), suggesting that these contaminants observed in Figure 2 (cytochrome and semiquinone species) had been removed during the purification process. The specific activity of pMMO^{c} using duroquinol as a reductant was ≈ 50 nmol of propylene oxide produced/min per mg. The type 2 Cu^{2+} EPR signals observed could be simulated with the following

Table 3 Comparison of EPR parameters of the cupric sites in pMMO isolated from various methanotrophs

Species and reference	EPR parameter			
	$g_{\parallel}$	$g_{\perp}$	$A_{\parallel}^{Cu}$ (mT)	A^{N} (mT)
M. capsulatus (Bath) [30]	2.26	2.06	18.0	–
Me. trichosporium OB3b [20]	2.24	2.06	18.4	–
M. capsulatus (Bath) [16]	2.25	2.06	18.1	–
Meth. album BG8 [29]*	2.243	2.067	18.0	1.8
Meth. album BG8 [29]†	2.251		18.0	1.8
M. capsulatus (Bath) [15]	2.244		18.5	1.9
M. capsulatus (Bath) [15]	2.246		18.0	1.9
M. capsulatus (Bath) (this study)	2.24	2.06	18.5	1.5

* This was assigned to Cu^{2+} co-ordinated by 3–4 histidines.

† This is a nearly identical Cu^{2+} site, presumably ligated by nitrogens from the peptide backbone.

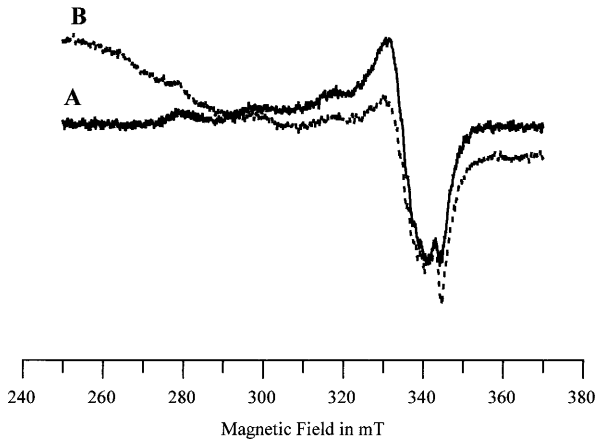

Figure 5 EPR spectra of the purified pMMO^{c} before and after addition of oxidant

X-band EPR spectra of the purified pMMO^{c} before (trace A, solid trace) and after (trace B, dotted trace) oxidation with 1 mM $K_3Fe(CN)_6$. Spectra were recorded at a microwave power of 100 μW, a modulation frequency of 100 kHz, a temperature of 9 K and a modulation amplitude of 0.5 mT.

values: $g_{\parallel} = 2.24$, $g_{\perp} = 2.06$, $A_{\perp}^{Cu} = 1$ mT and $A_{\parallel}^{Cu} = 18.5$ mT. The superfine coupling was around $A^{N} = 1.5$ mT assuming four equivalent nitrogens.

As expected, the *N*-superhyperfines were better resolved in the spectra of pMMO^{c} from *M. capsulatus* (Bath) cells grown in ^{63}Cu-enriched media than spectra of pMMO^{c} from cells grown in non-enriched copper media (Figure 3). The *N*-hyperfines were not as pronounced as expected, suggesting that the copper exchange may not be complete. There were some traces of the radical signal ($g = 2.0$) remaining in this sample.

The experimental spectrum of ^{63}Cu-labelled pMMO^{c} was compared with a simulation of a type 2 copper spectrum (Figure 4). It could be concluded from this that the seven-line pattern observed in the $g_{\perp}$ region in the EPR spectra of pMMO^{c} is consistent with spectra arising from an unpaired electron spin on a copper interacting magnetically with three/four nitrogens. This is consistent with data from others listed in Table 3 as well as the simulation by Yuan et al. [26,29] and Katterle et al. [43] of the Cu^{2+} site. It is clear that the spectra do not consist of a 10-line pattern arising from three equivalent $I = 3/2$ copper nuclei, as

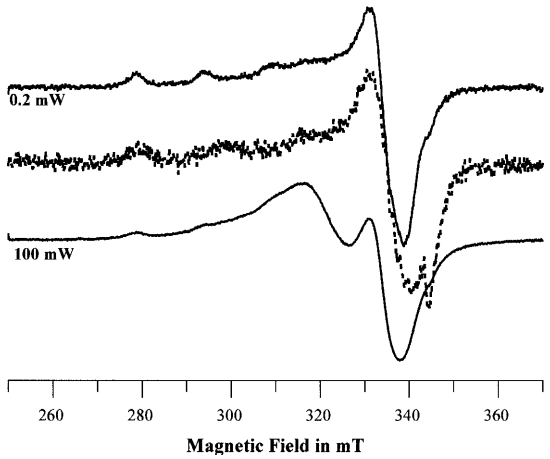

Figure 6 Effect of addition copper to Cu-depleted pMMO^{c}

EPR spectra of the pMMO^{c} before (dotted trace) and after (upper solid trace) addition of 157 μM copper, both measured at 0.2 mW. There was a slight change of $g_{\parallel}$ and $g_{\perp}$. The lower solid trace was measured at 100 mW. All spectra were recorded at a temperature of 10 K, modulation frequency of 100 kHz and a modulation amplitude of 0.5 mT.

would be expected for a trinuclear copper cluster model as proposed by Chan and co-workers [11,16–18]. Microwave power saturation studies at several temperatures (4–50 K) of our pMMO^{c} preparation was tried, but it was practically impossible to get reasonable fits [40], indicating an inhomogeneity in the EPR-active Cu^{2+} site. Nevertheless, the $P_{1/2}$ value at 4 and 10 K for pMMO^{c} can be estimated to be 100–150 μW. The relaxation properties of the EPR-active Cu^{2+} in pMMO membranes [43] or in whole cells [15] and in our pure pMMO^{c} preparation is consistent with a mononuclear Cu^{2+} EPR-active site.

Possible oxidation of pMMO^{c} by $K_3Fe(CN)_6$

Chan and co-workers [16,17] found that pMMO preparations oxidized by ferricyanide [$K_3Fe(CN)_6$] gave EPR spectra with an unusual broad quasi-isotropic signal, which they proposed to originate from an exchange-coupled trinuclear copper cluster. The intensity of their EPR signal was found to be consistent with the oxidation of 15 copper ions. However, treatment of pMMO-containing membrane fractions from *Meth. album* BG8 with $K_3Fe(CN)_6$ resulted in an EPR signal that was attributed to a $CuFe(CN)_6^{2-}$ complex and not an intrinsic trimeric copper cluster [27]. Attempts to oxidize our pMMO^{c} preparation resulted in little or no change in the intensity of the Cu^{2+} EPR signal, the decrease observed being that due to dilution (Figure 5). The broad peak around 250 mT is due to $Fe(CN)_6^{3-}$. Consequently the concentration did not increase by a factor of 2–3 and did not produce the unusual isotropic copper EPR spectrum. Possible reasons for this signal have been proposed to be copper-binding cofactors [30], a $K_2CuFe(CN)_6$ complex [27] or adventitiously bound copper ions, as we demonstrate in Figures 6 and 7. The latter proposal is substantiated by the fact that when 157 μM Cu^{2+} ions was added to pMMO^{c}, the resultant spectrum (Figure 6) was similar to the oxidized spectra of pMMO samples observed by Chan and co-workers [11,16,17]. These results indicate that there are no easily oxidizable copper ions or that any trinuclear cluster is present in the pMMO^{c}.

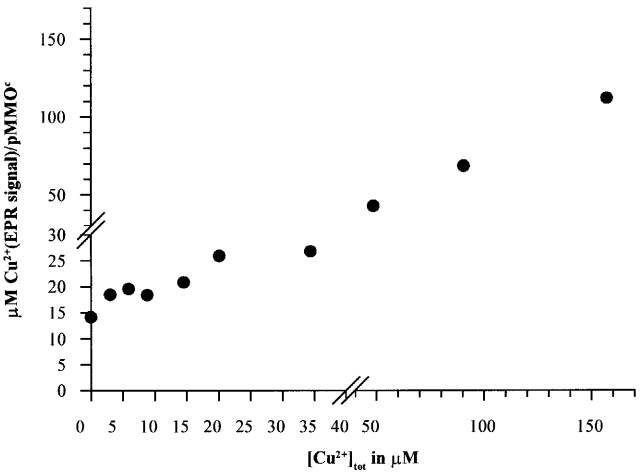

Figure 7 Cu^{2+} titration of EDTA-treated pMMO^c

$CuSO_4$ was sequentially added to EDTA-treated pMMO^c (5 mg/ml) to give the final Cu^{2+} concentrations shown on the *x* axis. The [Cu^{2+}] was determined by integration of the EPR signal. The EDTA-treated pMMO^c samples contained 14 μM copper.

Concentration of copper ions in pMMO^c

Chan and co-workers [17] suggested that pMMO membranes contained $\approx$ 20 Cu atoms per pMMO molecule. This was found to be similar to the stoichiometry found in their purified pMMO [16], which comprised of 15 copper ions arranged into five trinuclear copper clusters. These clusters were classified as having either an electron-transfer (E) or a catalytic (C) function. They also proposed that the amount of adventitiously bound copper associated with pMMO membranes was minimal.

ICP-ES analysis was used to obtain the total concentration of metal ions in pMMO^c in conjunction with EPR and some activity measurements (Table 4). After pMMO^c was treated with 10 mM EDTA followed by Sephadex G-25 column chromatography to remove excess metal–EDTA complexes, the ICP-ES measurements (Table 4) showed that the total concentration of copper ions decreased by 2.5-fold to 0.01 μmol/mg. The concentration of total iron did not notably decrease after EDTA treatment. The specific activity of the pMMO^c decreased by 50 %, suggesting that the copper ions removed were essential for maximal activity. When the EDTA-treated pMMO^c sample was analysed by EPR (Figure 6, dotted trace) there was no drastic change in the cupric signal although the *N*-superhyperfines were somewhat better resolved (results not shown), indicating that some adventitious EPR-active Cu^{2+} ions and EPR-silent copper ions, necessary for maximal enzyme activity, were removed (Table 4).

The effect of copper addition to the EDTA-treated pMMO^c was examined to see if the added copper would undergo magnetic interaction therefore supporting the trinuclear copper cluster hypothesis. The EDTA-treated pMMO^c sample was estimated to have $\approx$ 14 μM Cu^{2+} ions by integration of the copper signal at the beginning of the copper titration experiment. The addition of Cu^{2+} ions was correlated with the concentration of Cu^{2+} ions that could be calculated by integration of the corresponding EPR signal. Thus any magnetic interaction of the copper ions to form a trinuclear cluster would result in a lower-intensity cupric signal than would be expected from the amount of Cu^{2+} ions added.

From Figure 7 it can be concluded that the addition of copper ions resulted in two distinct phases. In the first phase addition of up to 25 μM copper resulted in an increase in the Cu signal with 12 μM being EPR-detectable, indicating that about 50 % of the added Cu was EPR-silent. In the EDTA-treated sample only 0.3 copper ions/subunit were EPR-active out of a total of 1 Cu/subunit. This could be consistent with a trinuclear cluster in which one atom of copper out of three would be EPR-active. To obtain 1 EPR-active copper atom/subunit it was observed that a total 1.9 Cu/subunit were present in the protein. It would have been necessary to have three copper ions to have been consistent with a trinuclear cluster. That the activity of pMMO is restored with Cu^{2+} addition after treatment of membrane preparations with EDTA or diethyldithiocarbamate ('DDTC') is well-documented [20,21,25] and in agreement with our result that we can restore 1 specific EPR-active Cu^{2+}/subunit by addition of copper.

In the second phase, starting from when $\approx$ 40–50 μM Cu^{2+} was added, all the added copper was EPR-active and a distinct and heterogeneous EPR signal (as exemplified by its power-saturation behaviour) was observed in addition to the well-resolved EPR signal (Figures 3 and 6). The characteristics of this species (after the addition of an extra 157 μM copper) are such that it can be distinguished from the well-resolved pMMO^c Cu site signal in that the *g* values are shifted slightly and the linewidth or *A* value is narrower (Figure 6). Furthermore, this Cu^{2+} species showed no resolution of the *N*-superhyperfine coupling and can be readily removed on a Sephadex G2-5 column, yielding the pMMO^c Cu^{2+} site EPR spectrum with the

Table 4 Copper and iron metal analyses and activity of purified pMMO complex

Values in parentheses show the number of copper atoms/protein molecule assuming a molecular mass of 104 kDa, as estimated from protein sequences available on the NCBI database (http://www.ncbi.nlm.nih.gov) under accession number L40804. Specific activity was measured in the presence of 50 μM $CuSO_4$. Metal ion analysis was performed on buffer alone and deducted from sample values. Unless otherwise stated data are from this study.

	Metal analysis (μmol/mg; per monomer)				Specific activity (nmol of propylene oxide/min per mg)
Protein sample	Cu/protein	EPR-active Cu/protein	Fe/protein	EPR-active Fe/protein	
pMMO [16]	0.133–0.141 (15)		0		2.6–5.1
pMMO^c (as isolated)	0.025 (2.4)	0.0006–0.0008 (0.6–0.8)	0.011 (1)	0	30–50
pMMO^c + 10 mM EDTA	0.010 (1)	0.0028 (0.3)	0.009 (0.9)	0	15
EDTA sample + 25 μM Cu^{2+}	0.014 (1.5)	0.0054 (0.5)	0.009 (0.9)	0	
EDTA sample + 44 μM Cu^{2+}	0.019 (1.9)	0.001 (1)	0.009 (0.9)	0	
pMMO^c + PMS + ascorbate			0.011 (1)	Cannot be quantified	
pMMO^c + PMS + dithionite			0.011 (1)	0.0066 (0.6)	

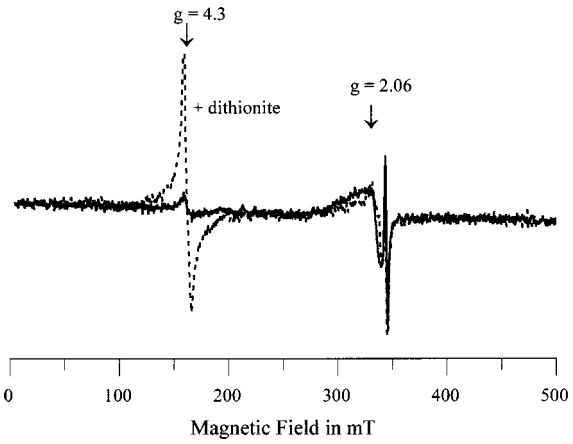

Figure 8 Effect of reductant on pMMO^c

X-band EPR spectra of the ferric site of pMMO^c after reduction by ascorbate (solid trace) and dithionite (dotted trace). The anaerobic sample pMMO^c was reduced with 1 mM ascorbate or 1 mM sodium dithionite in the presence of the mediator PMS (100 μM). The radical signal at $g = 2$ is due to PMS. The spectra were recorded at a microwave power of 1 mW, a temperature of 4 K, a modulation frequency of 100 kHz and a modulation amplitude of 0.5 mT.

resolved hyperfine structure. The extra adventitious and loosely bound copper was superimposed on the pMMO^c cupric site, making it difficult to distinguish the environment of the coppers based on analysis of the copper hyperfines and g values. Interestingly, this spectrum was similar to the oxidized pMMO sample spectra observed by Chan and co-workers [16–18], especially when using 100 mW microwave power instead of under non-saturating conditions (Figure 6, lower trace with extra 157 μM copper). This indicates that if the concentration of EPR-active copper is unusually high (over 1/subunit) then the samples start to manifest the broad isotropic signal thought to be trinuclear copper clusters by Chan and co-workers. This artificial broad isotropic signal might well be a trinuclear cluster, but it is not relevant to the active site of pMMO and is probably due to a non-specifically bound copper complex.

The total amount of copper and iron in the EDTA-treated sample was 1 Cu/subunit and 1 Fe/subunit. Doubling this amount of copper (Table 4) leads to a 2–3-fold increase in the specific activity. If the 2-fold increase in the activity required the formation of trinuclear clusters then at least a 3-fold increase in the amount of copper should have been found in the protein. In the EDTA-treated pMMO^c sample the copper concentration deduced by integration of the cupric EPR signal (0.003 μmol/mg of protein) was $\approx$ 3-fold lower than the concentration of copper as calculated by ICP-ES (0.01 μmol/mg of protein). This could indicate that for every EPR-detectable Cu^{2+} there is a maximum of $\approx$ 2 EPR-silent copper ions, whereas in the copper-titration experiment it was necessary to have a total of 1.9 copper atoms/subunit to obtain one EPR-active Cu^{2+}/subunit. The extra 0.9 Cu could exist as Cu^+ ions or be magnetically coupled in a cluster. We observed lower amounts of EPR-silent copper, one per EPR-active Cu^{2+}, than other reports [27]. Yuan et al. [27] also concluded that the enzyme (47, 27 and 25 kDa) comprised four coppers ions whereas we believe that there is probably one but no more than two EPR-silent coppers/EPR-active copper. Taken together, the EPR simulations, the Cu^{2+} relaxation properties, the oxidation attempts, the low copper content and absence of broad isotropic Cu^{2+} EPR species strongly suggest that the EPR-visible Cu^{2+} in pure pMMO is mononuclear and could have an electron-transport role.

The role of iron in pMMO^c

Purified pMMO^c contains 1 iron atom/subunit. To determine if this iron was similar to that observed in the sMMO di-iron–oxygen cluster [44] we attempted to evaluate conditions that would result in an EPR-visible species of this type of cluster. The mixed-valency form [Fe(III)Fe(II)] can readily be obtained in sMMO after incubation in the presence of the redox mediator PMS and a reductant such as ascorbate or dithionite. This species normally has a strong $S = 1/2$ EPR signal specific for this type of cluster, with all g values below $g = 2.0$ [44]. After incubation with PMS and ascorbate (see the Materials and methods and Figure 8, solid trace) no mixed-valency di-iron cluster signal was observed and the Cu^{2+} EPR signal decreased. Interestingly there was a small but significant increase in the $g = 4.3$ signal. This could be due to Fe^{3+} interacting with another paramagnetic species in the oxidized state, thus making it EPR-silent. Upon reduction with ascorbate/PMS, the unidentified species was reduced, thus eliminating the magnetic interaction with the rhombic Fe^{3+} and making it EPR-active. Further reduction of pMMO^c with dithionite/PMS gave no indication of the presence of a mixed-valency or diferrous di-iron cluster [44], or the presence of an iron–sulphur cluster [45]. The spectrum of the reduced pMMO^c gave an unexpected and dramatic increase in a symmetrical and isotropic signal at $g = 4.3$; the sharpness and the isotropic nature of this signal is characteristic of specifically bound Fe^{3+} ions in an octahedral ligation environment (Figure 8, dotted trace). This type of EPR signal is from the middle Kramers doublet of ferric high spin $S = 5/2$ centre, with an $|E/D|$ value of 0.33 [45]. The concentration of Fe^{3+} ions in pMMO^c was estimated to be $\approx 33 \pm 6$ μM by integration of the Fe^{3+} EPR signal against transferrin (Table 4) at two temperatures.

Thus the increase in the Fe^{3+} signal upon reduction indicates that the normally resting Fe^{3+} interacts magnetically with another species, yielding an EPR-silent Fe^{3+} site. The microwave-power-saturation behaviour of this novel pMMO^c Fe^{3+} site at 4 and 6.5 K was identical to that of transferrin with an Fe^{3+}–tyrosinate ligation (results not shown). Transferrin has Fe^{3+} strongly bound in an octahedral environment thus giving a rhombic Fe^{3+} EPR signal. Since Fe^{3+} in transferrin has the same magnetic behaviour and g value as the iron centre in pMMO^c following reduction, it strongly suggests that the Fe^{3+} in pMMO^c exists in a similar ligating environment. Clearly this Fe^{3+} site, after reduction, is different from the known di-iron clusters [44] or iron–sulphur proteins [45] and must be of a different novel type. If this Fe^{3+} was co-ordinated to tyrosine it would explain why it is not reduced under these reductive conditions, as several iron–tyrosinate proteins are difficult to reduce [46,47]. The incubation with dithionite resulted in a decrease in the amount of EPR-visible copper but not complete reduction of the Cu^{2+} ions, as was observed by Nguyen et al. [17].

The presence of iron has also been previously observed in purified pMMO samples from *M. capsulatus* (Bath) [30], *Me. trichosporium* OB3b [20] and *M. capsulatus* (strain M) membranes [10]. The iron is largely EPR-silent and could only be observed after the formation of a ferrous NO derivative ($g = 4.03$), which could also be observed in the related ammonia mono-oxygenase from *Nitrosomonas europaea* membranes [48]. Our preliminary experiments have not reproduced this iron–NO complex. A broad EPR signal at $g = 12.5$ from oxidized pMMOH, characteristic of a magnetically coupled iron centre, has been reported

in pMMO [30] but we have not observed this signal either. Their signal might well be a denatured form of an iron cluster. Therefore, in addition to the one EPR-active mononuclear copper site and possibly one EPR-silent copper site there appears to be 1 Fe/subunit in active pMMO. The EDTA-treated pMMO showed that iron was tightly bound or not accessible to EDTA, perhaps an indication that it is part of the active site.

Possible explanations for an EPR-silent Fe^{3+} ion could be that it is exchange-coupled to another entity (Z) that can be reduced, as it is highly unlikely that the iron is in a stable Fe^{4+} state. Several different possibilities exist for Z, such as: (i) a Cu^{2+} species; (ii) another Fe^{3+} species; (iii) one other paramagnetic metal ion such as Mn or (iv) a radical species such as tyrosyl or tyrosyl-derived radical as found in the copper enzyme galactose oxidase [49] or close to the Cu_{a3} in cytochrome *c* oxidase [50]. The putative radical should then interact magnetically with the iron.

Conclusions

We have developed a novel purification method yielding a duroquinol-driven particulate methane-oxidizing complex (pMMO^e) with the highest activity recorded so far. This pMMO^e contains one EPR-silent iron and an EPR-active copper ion, which is probably part of an electron-transfer complex and independent of the oxygen-activating site. These findings give us a greater insight into the *in vivo* mechanism of an active pMMO^e.

We would like to thank the Biotechnology and Biological Sciences Research Council for financial support (to P.B.). This study was also supported by the European Commission through the Training and Mobility of Researchers programme for the Iron-Oxygen Protein Network (grant no. FMRXCT98-0207) to K.K.A. and H.D. and the Research Council of Norway to K.K.A. Electron microscopy was carried out in collaboration with Dr A. Kitmitto and Dr R. Ford at the University of Manchester, Institute of Science and Technology (UMIST), Manchester, U.K. Electrospray ionization MS was carried out by Dr A. Holberg and Dr E. Adeosun (University of Warwick, Coventry, U.K.). N-terminal sequencing analysis was performed by Dr A. Moir (University of Sheffield, Sheffield, U.K.). We are grateful to Dr S. Charlton (University of Warwick) for the provision of ^{63}Cu-labelled cells.

REFERENCES

1 Stanley, S. H., Prior, S. D., Leak, D. J. and Dalton, H. (1983) Copper stress underlies the fundamental change in intracellular location of methane monooxygenase in methane-oxidising organisms: studies in batch and continuous cultures. Methane monooxygenase from *Methylosinus trichosporium* OB3b. Biotechnol. Lett. **5**, 487–492

2 Fox, B. G., Froland, W. A., Dege, J. E. and Lipscomb, J. D. (1989) Methane monooxygenase from *Methylosinus trichosporium* OB3b. Purification and properties of a 3-component system with high specific activity from a type-II methanotroph. J. Biol. Chem. **264**, 10023–10033

3 Green, J. and Dalton, H. (1985) The biosynthesis and assembly of protein A of soluble methane monooxygenase from *Methylococcus capsulatus* (Bath). J. Biol. Chem. **260**, 15795–15801

4 Green, J. and Dalton, H. (1988) Protein B of soluble methane monooxygenase from *Methylococcus capsulatus* (Bath). A novel regulatory protein of enzyme activity. J. Biol. Chem. **263**, 17561–17565

5 Liu, K. E. and Lippard, S. J. (1991) Redox properties of the hydroxylase component of methane monooxygenase from *Methylococcus capsulatus* (Bath). Effects of protein B, reductase, and substrate. J. Biol. Chem. **266**, 12836–12839

6 Wallar, B. J. and Lipscomb, J. D. (1996) Dioxygen activation by enzymes containing binuclear non-heme iron clusters. Chem. Rev. **96**, 2625–2657

7 Lund, J. and Dalton, H. (1985) Further characterisation of the FAD and Fe_2S_2 redox centers of component C, the NADH:acceptor reductase of the soluble methane monooxygenase of *Methylococcus capsulatus* (Bath). Eur. J. Biochem. **147**, 291–296

8 Nakajima, T., Uchiyama, H., Yagi, O. and Nakahara, T. (1992) Purification and properties of a soluble methane monooxygenase from *Methylocystis*. Biosci. Biotech. Biochem. **56**, 736–740

9 Pilkington, S. J. and Dalton, H. (1991) Purification and characterisation of the soluble methane monooxygenase from *Methylosinus sporium* 5 demonstrates the highly conserved nature of this enzyme in methanotrophs. FEMS Microbiol. Lett. **78**, 103–108

10 Akent'eva, N. F. and Gvozdev, R. I. (1988) Purification and physicochemical properties of methane monooxygenase from membrane structures of *Methylococcus capsulatus*. Biokhimiya **53**, 91–96

11 Chan, S. I., Nguyen, H.-H. T., Shiemke, A. K. and Lidstrom, M. E. (1993) Biochemical and biophysical studies toward characterization of the membrane-associated methane monooxygenase. In Microbial Growth on C_1 Compounds (Murrell, J. C. and Kelly, D. P., eds.), pp. 107–127, Itercept, Andover

12 Cook, S. A. and Shiemke, A. K. (1996) Evidence that copper is a required cofactor for the membrane-bound form of methane monooxygenase. J. Inorg. Biochem. **63**, 273–284

13 Elliott, S. J., Randall, D. W., Britt, R. D. and Chan, S. I. (1998) Pulsed EPR studies of particulate methane monooxygenase from *Methylococcus capsulatus* (Bath): evidence for histidine ligation. J. Am. Chem. Soc. **120**, 3247–3248

14 Gvozdev, R. I., Shushenacheva, E. V., Pylyashenko-Novochatnii, A. I. and Belova, V. S. (1984) Investigation of enzymatic oxidation by methane monooxygenase of *Methylococcus capsulatus*, strain M, membrane structure. Oxidation Com. **7**, 249–266

15 Lemos, S. S, Collins, M. L. P., Eaton, S. S., Eaton, G. R. and Antholine, W. E. (2000) Comparison of EPR-visible Cu^{2+} sited in pMMO from *Methylococcus capsulatus* (Bath) and *Methylomicrobium album* BG8. Biophys. J. **79**, 1085–1094

16 Nguyen, H.-H. T., Elliot, S. J., Yip, J. H.-K. and Chan, S. I. (1998) The particulate methane monooxygenase from *Methylococcus capsulatus* (Bath) is a novel copper-containing three-subunit enzyme. Isolation and characterization. J. Biol. Chem. **273**, 7957–7966

17 Nguyen, H.-H. T., Nakagawa, K. H., Hedman, B., Elliot, S. J., Lidstrom, M. E., Hodgson, K. O. and Chan, S. I. (1996) X-ray absorption and EPR studies on the copper ions associated with the particulate methane monooxygenase from *Methylococcus capsulatus* (Bath), Cu(I) ions and their implications. J. Am. Chem. Soc. **118**, 12766–12776

18 Nguyen, H.-H. T., Shiemke, A. K., Jacobs, S. J., Hales, B. J., Lidstrom, M. E. and Chan, S. I. (1994) The nature of the copper ions in the membranes containing the particulate methane monooxygenase from *Methylococcus capsulatus* (Bath). J. Biol. Chem. **269**, 14995–15005

19 Nguyen, H.-H. T., Zhu, M., Elliot, S. J., Nakagawa, K. H., Hedman, B., Costello, A. M., Peeples, T. L., Wilkinson, B., Morimoto, H., Williams, P. G. et al. (1996) The biochemistry of the particulate methane monooxygenase. In Microbial Growth on C_1 Compounds (Lidstrom, M. E. and Tabita, F. R., eds.), pp. 150–158, Kluwer Academic Publishers, Dordrecht

20 Takeguchi, M., Mijakawa, K., Kamachi, T. and Okura, I. (1997) Purification and properties of particulate methane monooxygenase from *Methylosinus trichosporium* OB3b. J. Inorg. Biochem. **67**, 278–279

21 Takeguchi, M., Miyakawa, K. and Okura, I. (1998) Purification and properties of particulate methane monooxygenase from *Methylosinus trichosporium* OB3b. J. Mol. Cat. A: Chem. **132**, 145–153

22 Takeguchi, M., Miyakawa, K. and Okura, I. (1998) Properties of the membranes containing the particulate methane monooxygenase from *Methylosinus trichosporium* OB3b. Biometals **11**, 229–234

23 Tonge, G. M., Harrison, D. E. F. and Higgins, I. J. (1977) Purification and properties of the methane monooxygenase system from *Methylosinus trichosporium* OB3b. Biochem. J. **161**, 333–344

24 Tonge, G. M., Harrison, D. E. F., Knowles, C. J. and Higgins, I. J. (1975) Properties and partial purification of the methane-oxidising enzyme systems from *Methylosinus trichosporium*. FEBS Lett. **58**, 293–299

25 Tukhvatullin, I. A., Korshunova, L. A., Gvozdev, R. I. and Dalton, H. (1996) Investigation of the copper center of membrane-bound methane monooxygenase from subcellular structures of *Methylococcus capsulatus* (strain M). Biochemistry (Moscow) **61**, 886–891

26 Yuan, H., Collins, M. L. P. and Antholine, W. E. (1997) Low frequency EPR of the copper in particulate methane monooxygenase from *Methylomicrobium albus* BG8. J. Am. Chem. Soc. **119**, 5073–5074

27 Yuan, H., Collins, M. L. P. and Antholine, W. E. (1998) Concentration of Cu EPR-detectable Cu, and formation of cupric-ferrocyanide in membranes with pMMO. J. Inorg. Biochem. **72**, 179–185

28 Yuan, H., Collins, M. L. P. and Antholine, W. E. (1998) Analysis of type 2 Cu(2+) in pMMO from *M. album* BG8. Biophys. J. **74**, 217–271

29 Yuan, H., Collins, M. L. P. and Antholine, W. E. (1999) Type 2 Cu(2+) in pMMO from *Methylomicrobium album* BG8. Biophys. J. **76**, 2223–2229

30 Zahn, J. A. and DiSpirito, A. A. (1996) Membrane-associated methane monooxygenase from *Methylococcus capsulatus* (Bath). J. Bacteriol. **178**, 1018–1029

31 Smith, D. D. S. and Dalton, H. (1989) Solubilization of methane monooxygenase from *Methylococcus capsulatus* (Bath). Eur. J. Biochem. **182**, 667–671

32 DiSpirito, A. A., Gulledge, J., Shiemke, A. K., Murrell, J. C., Lidstrom, M. E. and Krema, C. L. (1992) Trichloroethylene oxidation by the membrane-associated methane monooxygenase in type I, type II, and type X methanotrophs. Biodegradation **2**, 151–164

33 Prior, S. D. and Dalton, H. (1985) Acetylene as a suicide substrate and active site probe for methane monooxygenase from *Methylococcus capsulatus* (Bath). FEMS Microbiol. Lett. **29**, 105–109

34 Shiemke, A. K., Cook, S. A., Miley, T. and Singleton, P. (1995) Detergent solubilization of membrane-bound methane monooxygenase requires plastoquinol analogs as electron donors. Arch. Biochem. Biophys. **321**, 421–428

35 Prior, S. D. and Dalton, H. (1985) The effect of copper ions on membrane content and methane monooxygenase activity in methanol-grown cells *Methylococcus capsulatus* (Bath). J. Gen. Microbiol. **131**, 155–163

36 Takeguchi, M., Fukui, K., Ohya, H. and Okura, I. (1999) Electron spin-echo envelope modulation studies on copper site of particulate methane monooxygenase from *Methylosinus trichosporium* OB3b. Chem. Lett. **7**, 617–618

37 Whittenbury, R., Phillips, K. C. and Wilkinson, J. F. (1970) Enrichment, isolation and some properties of methane-utilising bacteria. J. Gen. Microbiol. **61**, 205–218

38 Bradford, M. M. (1976) A rapid and sensitive method for the quantitation of microgram quantities of protein utilising the principle of protein-dye binding. Anal. Biochem. **72**, 248–254

39 Lowry, O. H., Rosebrough, N. J., Farr, A. L. and Randall, R. J. (1951) Protein measurement with the Folin phenol reagent. J. Biol. Chem. **193**, 265–275

40 Sahlin, M., Petterson, L., Gräslund, A., Ehrenberg, A., Sjöberg, B. M. and Thelander, L. (1987) Magnetic interaction between the tyrosyl free radical and the antiferromagnetically coupled iron center in ribonucleotide reductase. Biochemistry **26**, 5541–5548

41 Brusseau, G. A., Tsien, H.-C., Hanson, R. S. and Wackett, L. P. (1990) Optimization of trichloroethylene oxidation by methanotrophs and the use of a calorimetric assay to detect soluble methane monooxygenase activity. Biodegradation **1**, 19–29

42 Tate, S. and Dalton, H. (1999) A low molecular-mass protein from *Methylococcus capsulatus* (Bath) is responsible for the regulation of formaldehyde dehydrogenase activity *in vivo*. Microbiology **145**, 159–167

43 Katterle, B., Gvozdev, R. I., Abudu, N., Ljones, T. and Andersson, K. K. (2002) CW ENDOR study on the Cu^{2+} sites of particulate methane monooxygenase of *Methylococcus capsulatus* (strain M) and dopamine β-monooxygenase from bovine adrenal medulla. Biochem. J. **363**, 677–686

44 Andersson, K. K and Gräslund, A. (1995) Diiron-oxygen proteins. In Advances in Inorganic Chemistry, vol. 43 (Sykes, A. G., ed.), pp. 359–408, Academic Press, Orlando

45 Hagen, W. R. (1992) EPR spectroscopy of iron-sulfur proteins. In Advances in Inorganic Chemistry, vol. 38 (Sykes, A. G., ed.), pp. 165–222, Academic Press, Orlando

46 Que Jr, L. and Ho, R. Y. N. (1996) Dioxygen activation by enzymes with mononuclear non-heme iron active sites. Chem. Rev. **96**, 2607–2624

47 Que Jr, L. (1983) Metalloproteins with phenolate coordination Coordin. Chem. Rev. **50**, 73–108

48 Zahn, J. A., Arciero, D. M., Hooper, A. B. and DiSpirito, A. A. (1996) Evidence for an iron center in the ammonia monooxygenase from *Nitrosomonas europaea*. FEBS Lett. **397**, 35–38

49 Gerfen, G. J., Bellew, B. F., Griffin, R. G., Singel, D. J., Ekberg, C. A. and Whittaker, J. W. (1996) High-frequency electron paramagnetic resonance spectroscopy of the apogalactose oxidase radical. J. Phys. Chem. **100**, 16739–16748

50 MacMillan, F., Kannt, A., Behr, J., Prisner, T. and Michel, H. (1999) Direct evidence for a tyrosine radical in the reaction of cytochrome *c* oxidase with hydrogen peroxide. Biochemistry **38**, 9179–9184

Received 24 May 2002/16 September 2002; accepted 14 October 2002
Published as BJ Immediate Publication 14 October 2002, DOI 10.1042/BJ20020823